Vol. 13(2), pp. 10-22, July-December, 2022
DOI: 10.5897/JCEMS2021.0364
Article Number: DCA2C3F70078
ISSN: 2141-6605

http://www.academicjournals.org/JCEMS

ACADEMIC JOURNALS
expand your knowledge

Journal of Chemical Engineering and Materials Science

Full Length Research Paper

Computational fluid dynamics (CFD) simulation of a gas-solid fluidized bed: Residence time validation study

Baru Debtera

Chemical Engineering Department, College of Biological and Chemical Engineering,
Addis Ababa Science and Technology University, P. O. Box NO16417, Addis Ababa, Ethiopia.

Received 19 August, 2021; Accepted 8 March, 2022

In this work, the business Computational Fluid Dynamics (CFD) is used for the numerical simulations of an air-solid fluidized bed container in the solid phase involving a multi-fluid Eulerian multiphase model and the Kinetic Theory of Granular Flow (KTGF). The height of the fluidized bed setup is 1.5 m while its diameter is 0.2 m. With it, a series of experimentations were obtained using Helium tracer to determine the Residence Time Distribution (RTD) at various normalized velocities, that is, mixing of air-solids at different degrees. 2 and 3 dimensions of the fluidized bed container are simulated. The main purpose of this study is to understand the hydrodynamic behavior of air-solid fluidized bed container through a framework of Eulerian multiphase model and to analyze the hydrodynamic behavior of the air-solids mixing. As a first approach, the CFD model is validated using the experimental results of the residence time study. The numerical results of RTD corresponded well with the experimental findings. This shows that the CFD modeling might be used to indicate the performance of a fluidized bed reactor.

Key words: Computational fluid dynamics, fluidized bed, residence time distribution (RTD), gas-solids mixing, turbulence.

INTRODUCTION

Fluidization is the process whereby dense particles change into a fluid-like state over suspension in fluid. Fluidization entails delivering a flow of gas through a bed of granular substance at an adequate velocity, with the granulated bed being liquefied (Gidaspow, 1994; Richardson et al., 2008). Fluidized beds are common equipment in the industry and are used for catalytic reactions, increasing of size, element covering methods, heating system/chilling, drying, and mixing (Kunii and Levenspiel, 1991). Gas-solid fluidized beds are advantageous in many processes involving heat and/or mass transfer between phases. They provide efficient mixing, which results in excellent gas-solid contact and relatively uniform temperature/concentration profiles within the bed (Cui and Grace, 2007; Gidaspow, 1994). Indeed, the need for cleaner and sustainable energy source has led to the development of biomass gasifiers which employ fluidized bed technology. It is a hopeful tactic that specifies quick biomass central heating, effective heat, mass transfer and uniform reaction temperature (Salaices et al., 2012). Understandably, the physics behind fluidization indicates theimportance of

E-mail: baru.debtera@aastu.edu.et.

variable quantity such as pressure changes, minimum fluidization velocity, solid volume fraction profile, and particle velocity profile (Benzarti et al., 2012; Taghipour et al., 2005). Usually, fluidized bed reactors are chaotic in nature (Li et al., 2009). This is indicated by a turbulent fluidized bed. In addition, a fluidized bed is an intermediate that takes place in a chemical reaction involving gas and solid. The fluidized bed is mainly selected for the mixture of solid catalyzed gas segment reactions because it can regulate the temperature of the reaction zone well, and the situations in fluidized bed reactors are approximately isothermal.

Nowadays, Computational Fluid Dynamics (CFD) is a powerful device used for the complex phenomena amongst air and solid element segments in the fluidized bed. CFD can be used to solve Navier-Stokes equations and has become a helpful device for investigating and developing different flow systems. Computational properties have improved substantially with sharp declining expenses, allowing the acquisition of detailed computational information about reactions and flows at a fraction of the cost of the corresponding experiments (Dutta et al., 2010). It is possible to define a computational domain in which the geometry of the fluidized bed reactor can be incorporated and CFD approach can be used to solve the governing Navier-Stokes equations, using appropriate initial and boundary conditions. The results obtained from the numerical model can then be compared to experimental data for a necessary validation. Since computational assets have expanded significantly at forcefully diminishing costs, specified computational data about the flow can, these days, be acquired even with cheap experiments (Xia and Sun, 2002). The transient CFD simulations are performed to suggest the usability of the multiphase approach for the prediction of the solid phase mixing and residence time distribution in the riser (Andreux et al., 2008). Transient solution is always necessary because of the unsteady state nature of the fluidized bed. CFD is useful in understanding the quantitative hydrodynamics of fluidization and is needed for the design and scale-up of efficient reactors in several processes industries.

The systematic method used to estimate the performance of a supplier and inclusive mixing actions of a fluidized bed entails quantifying and examining the residence time distribution (RTD) of the solid segment (Pant et al., 2014). The gas mixing in circular fluidized bed risers is evaluated as an overall behavior. The total mixing conduct is considered by determining the set time delivery of a gas tracer inserted at the feed inlet. The knowledge of RTD function is very important for the optimization of the operating parameters and equipment configuration (Idakiev and Morl, 2013). The tracer is introduced at the inlet and monitored at the outlet of the column. The concentration of tracer is introduced as a pulse into a fluidized bed column at the feed inlet. Then, the samples are collected at the exit at fixed time intervals until tracer concentration goes to zero at the outlet (Lopez-Isunza, 1975). Using CFD, the flow of inert tracer units is determined using species transport equation, where the diffusion coefficient of elements, that is, the necessary parameter indicating particle diffusion capacity is investigated (Hua et al., 2014). Typically, a CFD study should be conducted on a pilot scale fluidized bed, and numerical methods are used as prototypes of the experimental arrangements and to confirm the experimental outcomes. The main goal of this effort is to use the CFD program available in ANSYS FLUENT application to simulate the hydrodynamic performance of a fluidized bed. A first approach of the full-fledged CFD model is important to prove the modeling through the investigational results presented. Due to the availability of residence time data, the CFD model is first validated with the RTD information obtained experimentally. The present study is divided into two main: validation of the two- and three-dimensions simulation of gas-solid fluidized bed with the RTD data and a subsequent study to identify the flow patterns of fluid-solid flow in the turbulent fluidized bed reactor. The numerically predicted RTD outcomes are associated through the experimental results of Lopez-Isunza (1975). The target is to make a meaningful comparison between the predictions of the RTD at three different airflow rates that give the normalized velocity $(U_0 / U_{mf} = 9.5; 8.0 \text{ and } 6.4)$. Note that the minimum fluidization velocity is 0.634 cm/s.

COMPUTATIONAL FLUID DYNAMICS (CFD) MODEL

Geometry and mesh

For the CFD simulations, initial mesh needs to be created. This mesh creates a geometry in which the calculations occur and furthermore is divided into several volumes according to the finite-volume methodology. These calculations are governed by the so-called Reynold's averaged Navier-Stokes (RANS) equations. Dimensions of the fluidized bed reactor (1.5 m height and a radius of 0.1 m) are simulated. The particle diameter used in the gas-solid fluidized bed is between 175 and 200 µm and falls in the Geldart group B particles (Geldart, 1973). The geometry is made in both 2D and 3D. The mesh consists of 12357 elements in 2D and 35616 elements in 3D, respectively. The mesh of the fluidized bed is as shown in Figure 1 as 2D and 3D.

As shown in Figure 1, the initial bed height is fixed at 0.5 m. The solid particles can be seen over the distributor plate. The gas inlet is at the bottom and the gas outlet is at the upper part. A tracer monitoring point is also at the top outlet.

Gas-solid model

For solutions in finite volume, an arrangement of balance

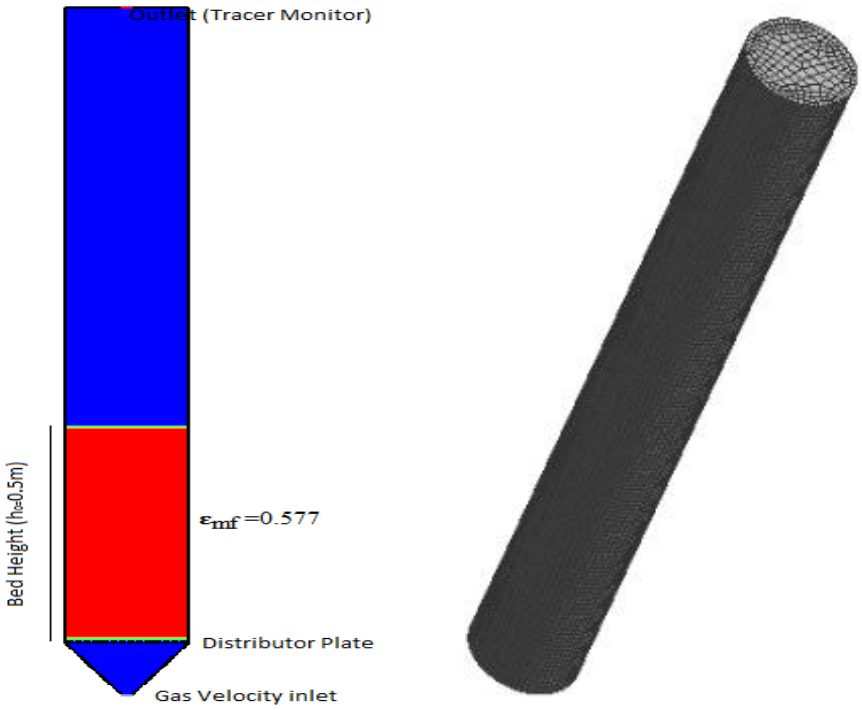

Figure 1. Mesh of the geometry of the fluidized bed reactor, as 2D and 3D, respectively.

equations is numerically solved for fluid flow over a number of control volumes, that is, over the so-called mesh cells. These balanced equations, calculated via the RANS approach for the conservation of mass, momentum and energy were used for CFD simulations. These equations are already implemented in the CFD software ANSYS Fluent® version 16.2. The CFD replication of the bed hydrodynamics is founded on the perception of Eulerian-Eulerian different phase flow prototypical incorporated in the kinetic theory of granular flow (KTGF) (Gidaspow et al., 2004; Tartan and Gidaspow, 2004). This engineering method invented since the theory for non-ideal dense gases was developed by Chapman and Cowling (1970) is used for nearby solid segment calculations. A brief explanation of the underlying theory related to KTGF is subsequently discussed.

Conservations of mass

The sum of volume fraction for gas and solid phases must be equal to unity:

$$\alpha_g + \alpha_s = 1 \quad (1)$$

where a subscript *g* and *s* stand for gas and solid phases.

The continuity equation for a gas phase and a solid phase are expressed as follows:

$$\frac{\partial}{\partial t}(\alpha_g \rho_g + \nabla.(\alpha_g \rho_g \vec{v}) = 0$$
$$\frac{\partial}{\partial t}(\alpha_s \rho_s + \nabla.(\alpha_s \rho_s \vec{v}) = 0 \quad (2)$$

Conservation of momentum

The momentum equation for the gas (g) phase is given as follows:

$$\frac{\partial}{\partial t}(\alpha_g \rho_g \vec{v}_g) + \nabla.(\alpha_g \rho_g \vec{v}_g \vec{v}_g) = -\alpha_g \nabla p + \nabla \bar{\bar{\tau}}_g + \alpha_g \rho_g \vec{g} - K_{gs}(\vec{v}_g - \vec{v}_s) \quad (3)$$

Momentum equation for solid phase:

$$\frac{\partial}{\partial t}(\alpha_s \rho_s \vec{v}_s) + \nabla.(\alpha_s \rho_s \vec{v}_s \vec{v}_s) = -\alpha_s \nabla p - \nabla p_s + \nabla \bar{\bar{\tau}}_s + \alpha_s \rho_s \vec{g} - K_{gs}(\vec{v}_g - \vec{v}_s) \quad (4)$$

Gas phase shear stress tensor, $\bar{\bar{\tau}}_g = \alpha_g \mu_g (\nabla \vec{v}_g + \overrightarrow{v_g^T})$ (5)

Solid phase shear stress tensor,

$$\bar{\bar{\tau}}_s = \alpha_s \mu_s (\nabla \vec{v}_s + \overrightarrow{v_s^T}) + \alpha_s (\lambda_s + \frac{2}{3}\mu_s) \nabla \vec{v}_s. \quad (6)$$

The solid phase stress tensor consists of a shear viscosity and a bulk viscosity; it arises from solid particle momentum exchange due to kinetics and collision. A frictional viscosity is considered for viscous-plastic translation. It occurs when a solid phase reaches the maximum volume fraction. The sum of collisional, kinetic and frictional viscosities gives the solids shear viscosity ($\mu_s = \mu_{s,col} + \mu_{s,kin} + \mu_{s,fr}$).

Solid collision viscosity (Syamlal et al., 1993):

$$\mu_{s,col} = \frac{4}{5}\alpha_s \rho_s d_p g_{o,ss}(1+e_{ss})(\Theta)_s^{1/2} \quad (7)$$

Solid kinetic viscosity (Syamlal et al., 1993):

$$\mu_{s,kin} = \frac{\alpha_s \rho_s d_p}{6(3-e_{ss})}\sqrt{\pi\Theta_s}\left[1+\frac{2}{5}\alpha_s g_{o,ss}(1+e_{ss})(3e_{ss}-1)\right] \quad (8)$$

Solid frictional viscosity (Schaeffer, 1987):

$$\mu_{s,fr} = \frac{p_s}{2\sqrt{I_{2D}}}\sin\varphi \quad (9)$$

where φ is the angle of internal friction.

Solid bulk viscosity (Lun et al., 1984):

$$\lambda_s = \frac{4}{3}\alpha_s \rho_s d_p g_{o,ss}(1+e_{ss})(\frac{\Theta}{\pi})_s^{1/2} \quad (10)$$

Solid pressure is implemented according to

$$p_s = \alpha_s \rho_s \Theta_s + 2\rho_s g_{o,ss}(1+e_{ss})\alpha_s^2 \Theta_s \quad (11)$$

Radial distribution function is implemented according to

$$g_{o,ss} = \left[1-(\frac{\alpha}{\alpha_{s,\max}})^{1/3}\right]_s^{-1} \quad (12)$$

where the restitution coefficient for particle-particle impacts, e_{ss} is static at 0.9 for all the simulations in the present work. This value is taken from literature studies (Balakin et al., 2012; Hu et al., 2010) on glass and polymer elements (in this study polymeric silica gel is used).

Wen-Yu and Gidaspow drag models are used for the momentum conversation coefficient. The Gidaspow effort model equation is a mixture of Wen-Yu and Ergun equations.

Drag function

$$K_{gs} = \frac{3}{4}C_D \frac{\alpha_g \alpha_s \rho_g}{d_p \alpha_g^{2.65}}\left|\vec{v}_g - \vec{v}_s\right| \quad (13)$$

Drag function (Gidaspow model, 1994):

$$K_{gs} = 150C_D \frac{\alpha_s \mu_g}{\alpha_g d_p^{2.}}(1-\alpha_g) + 1.75\frac{\alpha_g \rho_g}{d_p}\left|\vec{v}_g - \vec{v}_s\right| \quad \text{for } \alpha_g \le 0.8 \quad (14)$$

when $\alpha_g \ge 0.8$, Gidaspow drag model becomes Wen-Yu model.

$$C_D = \frac{24}{\alpha_g \mathrm{Re}_s}\left[1+(0.15\alpha_g \mathrm{Re}_s)^{0.687}\right]$$

and

$$\mathrm{Re}_s = \rho_g \frac{d_p}{\mu_g}\left|\vec{v}_g - \vec{v}_s\right|.$$

The coarse temperature is calculated by changeable kinetic energy equivalence for the particles, following the Kinetic Theory of Granular Flow (KTGF) belief. To require co×llisional energy dissipation, γ_s, outstanding to inelastic collisions of elements and the granular conductivity, K_s, the equation is given as:

$$\frac{3}{2}\left[\frac{\partial}{\partial t}(\alpha_s \rho_s \Theta) + \nabla \alpha_s \rho_s \Theta\right] = \bar{\tau} : \nabla \vec{V}_s + \nabla\left(K_s \nabla\Theta - \gamma_s\right) \quad (15)$$

$\Theta = \frac{1}{3}V_s^2$ is the granular temperature.

A list of sub-models used for the CFD model and their values are shown in Table 1. To simulate these equations inside the fluidized bed, various boundary conditions are required. The simulations in this study are done using gas phase (air) with density of 1.225 kg/m^3 and viscosity of 1.785×10^{-5} Pa s and solid phase with particle diameter between 175 and 200 µm, and density of 2400 kg/m^3. For tracer gas (Helium), the density and viscosity are 0.165 kg/m^3 and 2.0×10^{-5} Pa s, respectively.

Gas-solid mixing studies

Gas-solid fluidization is divided into several regimes depending on gas speed. In this study, the gas rate used falls within the bubble fluidized bed regime, that is, the range of Reynold number (Re) between 0.2 and 1000. Air bubbles increase in the fluidized bed; there is continuous transference of gas to the solid phase by diffusion and convection modes. The gas that enters the fluidized bed passes through the granular particles in the column. The bubble pushes through the bed of the solid particles and stops at the top. Accordingly, the bubble is like the cloud

Table 1. Summary of the numerically simulation boundary conditions and model parameters.

Descriptions	Sub-model
Granular viscosity	
Granular bulk viscosity	Lun et al. (2009)
Frictional viscosity	
Granular temperature	KTGF
Drag law	Gidaspow (1994)
Inlet boundary condition	Velocity inlet
Outlet boundary condition	Pressure outlet
Wall boundary condition	No slip for air
Parameter	**Values**
Bed height	0.5 m
Volume fraction of solid phase	0.577
Operating pressure	101325 Pa
Gas inlet velocity	(0.065, 0.051 and 0.041) m/s
Turbulent kinetic energy	0.30554 m^2/s^2
Turbulent dissipation rate	0.30553 m^2/s^3
Angle of internal friction	30°
Particle-particle restitution coefficient	0.9
Specularity coefficient for solid phase	0.001

of dense segment, in which the gas is continuously transferred by convection inside the bubble. In the cloud, the contact between solid and gas takes residence. This implies that air exists in the cloud, which flows back to the bubble again. Part of it might be exchanged with the solid phase by diffusion or adsorption with the solid that is exchanged with the emulsion phase. Convection and diffusion mechanisms of exchange occur simultaneously. The gas exchange among bubble and suspension phases has been described in terms of mass transfer coefficient by Kunii and Levenspiel (1991):

$$\frac{1}{\text{intrfacial area}}\frac{dN_A}{dt} = k\left(C_{Ab} - C_{Ae}\right) \quad (16)$$

where k is mass transfer coefficient (cm/s). Interchange rate is defined as,

$$\frac{1}{volume}\frac{dN_A}{dt} = k\left(C_{Ab} - C_{Ae}\right) \quad (17)$$

where k is mass transfer coefficient (s^{-1}).

Kunii and Levenspiel (1991) expected two transference steps, namely the transfer among bubble void and cloud particles intersection area and that between the cloud particles intersection area and the emulsion phase. They also presumed that the mass transfer quantity of bubble-cloud and cloud-emulsion is given as in terms of gas transfer quantity per unit volume of bubble void.

$$k_{bc} = 4.5\frac{u_{mf}}{D_b} + 5.85\left(\frac{D^{1/2}g^{1/4}}{D_b^{5/4}}\right) \text{ from bubble to cloud} \quad (18)$$

$$k_{ce} = 6.78\left(\frac{\alpha_{mf}u_b D_e}{D_b^{3}}\right)^{1/2} \text{ from cloud to emulsion} \quad (19)$$

They defined the overall gas transfer coefficient of the bubble phase and emulsion phase as follows:

$$k_b = \frac{k_{bc}k_{ce}}{k_{bc} + k_{ce}} \quad (20)$$

From the thorough information regarding the method of fluid (gas) in the cloud, it can carefully be expected that the gas structure in the cloud is roughly uniform. Chiba and Kobayashi (1970) used the analysis of Murray for the flow pattern around the spherical bubble to obtain the following expressions for the interchange coefficient:

$$k_b = \frac{6.78}{1-\alpha_g}\left(\frac{D\alpha_{mf}u_b}{D_b^{3}}\right) \quad (21)$$

Finally, Kobayashi et al. (1967) determined the rate of

exchange by measuring the RTD in a fluidized bed. They concluded that the interchange parameter could be expressed as:

$$k_b = \frac{11}{D_b}. \quad (22)$$

Equation 23 indicates that there is no effect of the diffusion coefficient of the transferring species, nor any direct effect of the fluid mechanical phenomen. However, in this study, Gidaspow and Wen-Yu gas-solid interchange coefficients are used to observe the conduct of the hydrodynamics in a fluidized bed.

Species transport model

Species transport equation is used for the residence time distribution (RTD) study. The conservation equation for the species predicts the residence mass portion of each species, Y_i, through the solution of a convection and diffusion equation from i^{th} species. The general conservation equation is given as follows:

$$\frac{\partial}{\partial t}(\rho_i) + \nabla.\left(\rho\vec{v}Y_i\right) = -\nabla\vec{J}_i + R_i + S_i \quad (23)$$

where ρ_i is density of species i, $\vec{v}$ is velocity vector, $\vec{J}i$ is diffusion change of species i, R_i is the net rate of creation of species by chemical reaction and S_i is the rate of creation by accumulation from the dispersed phase. In this situation, chemical reaction is not considered; therefore R_i and S_i are ignored and Equation 24 is reduced to:

$$\frac{\partial}{\partial t}(\rho_i) + \nabla.\left(\rho\vec{v}Y_i\right) + \nabla\vec{J}_i = 0 \quad (24)$$

where the diffusion flux of the species for turbulent flow is calculated by Fick's law and CFD uses the dilute estimate of Fick's law for prototypical mass diffusion due to the concentration difference and temperature. The diffusion flux might be given as follows:

$$\vec{J}_i = \nabla.Y_i\left(\rho D_{i,m} + \frac{\mu_t}{S_{ct}}\right) - D_{ti}\frac{\nabla T}{T} \quad (25)$$

where S_{ct} is the turbulent Schmidt number $S_{ct} = \frac{\mu_i}{\rho D_t}$ while the temperature gradient is negligible and combines Equations 25 and 26 form given as:

$$\frac{\partial}{\partial t}(\rho_i) + \nabla.\left(\rho\vec{v}Y_i\right) = \nabla.Y_i\left(\rho D_{i,m} + \frac{\mu_t}{S_{ct}}\right). \quad (26)$$

During the simulation, diffusion at the inlet is important because the pressure-based solver calculating the net exchanges of species at the inlets involves both convection and diffusion elements and compounds. That means the convection constituent is made static by the quantified inlet species mass fraction, while the diffusion factor depends on the difference of the calculated species' amount (which is not known priori).

Turbulent modeling

In various industrial processes related to fluidization, turbulence behavior is observed. k -ε model is the commonly used engineering turbulent classical for industrial applications; it is robust and reasonable accurate.

In this study, a standard k- ε model is used to calculate the transportation equation for turbulent kinetic energy (k) and dissipation rate of the turbulent kinetic energy (ε). The k-ε model is given as follows:

$$\nabla.(\rho_m k\vec{v}_m) = \nabla.(\frac{\mu_{t,m}}{\sigma_\varepsilon}\nabla k) + G_{k,m} - \rho_m\varepsilon \quad (27)$$

$$\nabla.(\rho_m k\vec{v}_m) = \nabla.(\frac{\mu_{t,m}}{\sigma_\varepsilon}\nabla k) + \frac{\varepsilon}{k}(c_{1\varepsilon}G_{k,m} - c_{2\varepsilon}\rho_m\varepsilon) \quad (28)$$

where $\mu_{t,m}$ is turbulent (eddy) viscosity computed from k – ε, ($\mu_{t,m} = \rho_m C_\mu \frac{k^2}{\varepsilon}$)

where C_μ=0.09, C_{e1}=1.44, C_{e2}=1.92, σ_ε=1 and $G_{k,m}$ is classical of turbulent kinetic energy due to velocity difference.

Residence time distribution (RTD)

Residence time distribution (RTD) study is significant to describe the mixing and flow rate patterns of the inner apparatus, and to determine whether the unit would be an ideal apparatus in the future, that is, tubular reactor or mixed flow reactor. Besides, RTD is used to prototype the reactor as a mixture of ideal reactors. Residence time distribution data values are used to investigate any non-idealities similar to directing, by transient and quick circuiting existing in the reactor (Levenspiel, 1999). It can also be used to measure up or to project a reactor once the kinetics is attained. To accomplish RTD replications, the transient examination of a tracer is measured with the same physical properties as that of incessant phase. The

transportation calculation for the mass flow rate of a turbulent flow can be written thus:

$$\frac{\partial}{\partial t}\left(\rho_m Y_{tr}\right)+\frac{\partial}{\partial x_j}\left(\rho_m \vec{v}_m Y_{tr}\right)=\frac{\partial}{\partial x_j}[\frac{\partial}{\partial x_j}Y_{tr}\left(\rho D_{i,m}+\frac{\mu_t}{S_{ct}}\right)] \quad (29)$$

where μ_t is a turbulent viscosity and is given as $\mu_t = \rho_m C_\mu \frac{k^2}{\varepsilon}$, and Y_{tr} is mass fraction of tracer species.

Numerical procedure for hydrodynamics

Mathematical method

ANSYS Fluent answers the main integral equations for mass conservation, conservation of momentum, kinetic theory of granular flow and turbulent simultaneously. This technique is used for finite volume approach for flow arrangements.

Pressure based problem solver method

Pressure-based calculation employs phase momentum equations, collective pressure, and calculations of phase volume fractions in a separate way. The phase uses an implicit technique for pressure connected equations (PC-SIMPLE). An extension of the SIMPLE system is established for polyphase flows. This consists of modifying the pressure and velocity which are functional to improve the limitation of the volume continuously.

Three or two dimensions discretization

Finite volume system used to conduct complex geometries is functional. The differentiation of the convective rate is first order exposed. Under transient formulation, the restricted second order implicit is used; this preparation would offer well stability, for time discretization to continuously confirm the bound variables. The bounded second order implicit is a better option for the fluidized bed to obtain stability and accurate results. A first order implicit transient design by means of the phase-Couple SIMPLE method is used to calculate the equations for both 2-dimensional and 3-dimensional cases.

Initial values and boundary values conditions

The initial condition might not influence the stable state solutions that may be favorable for the fluidized bed modeling. Notwithstanding, tactically estimate of initial conditions confirms the meeting of the solution. They are two kinds of initial conditions: solids volume fraction in the bed and Y-velocity of the air phase in the fluidized bed. The solid capacity fractions in the freeboard are initially set to zero (assuming only gas). The Y-velocity of the gas phase in the fluidized bed is computed completely with a steady state volumetric fluxes balance in which the flow rate going to the fluidized bed segment is linked to the volume flow rate leaving the fluidized bed segment (consisting of both solids and gas phase):

$$v_{in}u_{in} = v_g u_g \quad (30)$$

$$u_g = \frac{v_{in}u_{in}}{v_g} \quad (31)$$

The situations represent that the superficial velocity of the gas is a proportion of the bed volume to the feed inlet volume which is identical with the void fraction:

$$u_g = \frac{u_{in}}{\alpha_g} \quad (32)$$

Boundary conditions: At the inlet of the fluidized bed, there is gas superficial velocity for primary phase, while the secondary phase is zero inlet velocity. At the outlet of the fluidized bed there is atmospheric pressure. No slip, wall boundary condition is applied to the gas phase, while the partial slip condition is applied to the solid phase. A specularity coefficient (ϕ = 0.001) for a partial slip model is used based on the suggestion of Shi et al. (2015).

PROBLEM DESCRIPTION AND CFD METHOD

Problem identifications

Figure 1 is the conceptual representation of the fluidized bed that is modelled and simulated using software. This figure characterizes a cylindrical container, that is, the gas-solid fluidization bed with superficial air velocity inlet at the bottom of the column. The solid particles are patched with α_s =0.577 at the initial bed height (h_o) = 0.5 m. The fluidizing gas causes the gas-solids mixing. The gravitational effect on the particles bed is taken into account as the bed is vertical.

Simulation procedure

The assumption of the tracer does not involve any chemical reaction with the reactants to produce any product. The smallamount of tracer component has the same physical properties with the working fluid. That means the flow rate is not troubled inside the reactor after the tracer is presented. This assumption is used in many literature studies (Hua et al., 2014; Shilapuram et al., 2011). The RTD analysis such as mean residence time, change, and leaving age distribution can be done.

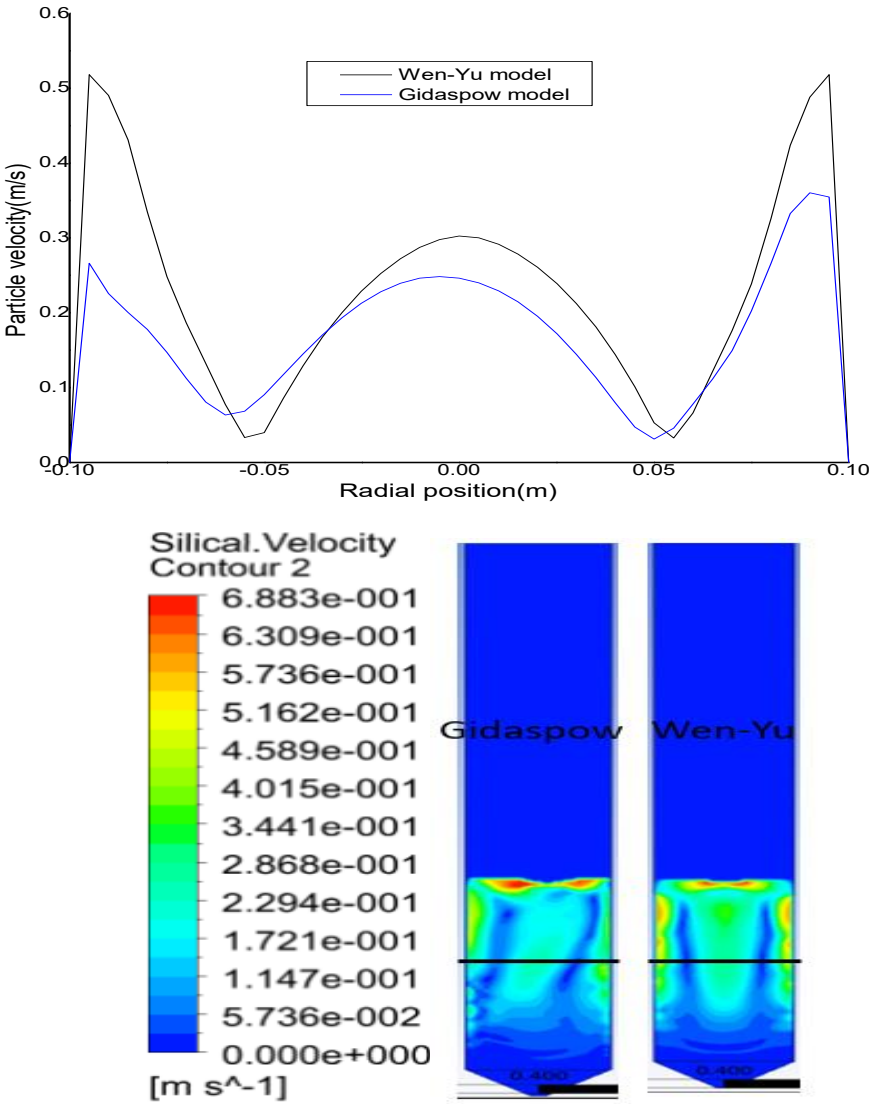

Figure 2. Time-averaged (10 s) simulation of solid particles (a) axial velocity along the radial height of 0.3 m and (b) velocity contour.

The tracer gas injection method involves:

(1) Firstly, run the steady state simulations for the flow rate and turbulence as shown in Table 1, for physical properties and boundary conditions. It may be noted that the residuals of the continuity, momentum, k-turbulent kinetic, $\mathcal{E}$- dissipation rate kinetic energy reduce in reaching steady state conditions.

(2) After it is achieved, it converges for the steady state simulation; the mass fraction of the tracer is made to 1 and the other equations are disabled. The tracer carries the properties of Helium gas, as mentioned in the experimental setup (Lopez-Isunza, 1975).

(3) Now the unsteady state equation for the tracer (Equation 29) is used for one iteration to imitate the Pulse method after which the mass fraction of the tracer is changed to 0.

(4) The flow equations (conservation of mass, conservation of momentum, k-turbulent kinetic, $\mathcal{E}$- dissipation rate kinetic energy species transport and tracer gas) are solved.

(5) Then, the mass density of the tracer is time monitored when leaving the fluidized bed.

RESULTS AND DISCUSSION

CFD reproductions of the fluidized bed are obtained by RTD validation study done by comparing the results with the experimental study done by Lopez-Isunza (1975).

Gas-solid hydrodynamics

Hydrodynamic characterization of gas-solid fluidized bed simulated by CFD in 2D with the drag equations of Gidaspow and Wen-Yu is done. Figure 2 represents the

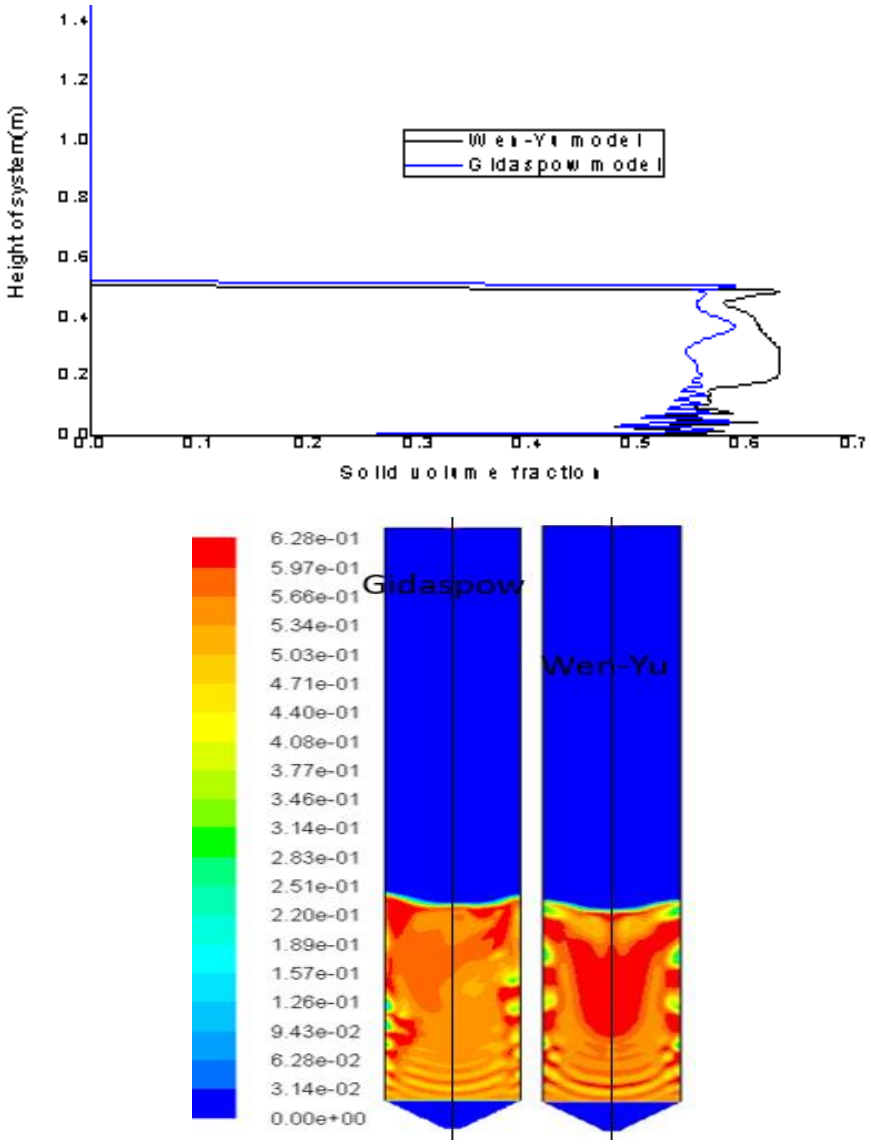

Figure 3. Time-averaged (10 s) simulation of solid particle volume fraction (a) that changed lengthways to center alliance of the fluidized bed and (b) contour in the fluidized bed.

time used for the solids velocity profile in the radial path at 0.3 m. The motoring height is chosen arbitrarily but care is taken to ensure that it is below the top elevation of the fluidized bed. This is done to ensure that the gas-solids mixing behavior is certainly investigated. It can be seen that the simulation results using Gidaspow and Wen-Yu gas-solid drag models are slightly different from each other. The solids axial velocity fluctuations along the radial position are larger in Wen-Yu model than in Gidaspow model. Experimental studies (Li et al., 2009; Loha et al., 2012) indicate that the variation in solids velocity is similar to that exhibited by Gidaspow drag model. This indicates that the Gidaspow model could be more accurate in predicting the gas-solid solid hydrodynamics in this study. Moreover, Gidaspow drag equation is a modified form of Wen-Yu (and Ergun) drag equations as explained earlier.

Figure 3 illustrates the time-averaged solid capacity fraction variation along the center of the fluidized bed. It shows the extreme solids volume fraction model equation of Wen-Yu (α_s = 0.63) compared to the model of Gidaspow (α_s = 0.59).

This specifies the Wen-Yu model equation promotes solids clustering as compared to the Gidaspow model. It is probably due to the huge gas velocity escaping along the walls thereby pushing the solid particle together and forming cluster. Figure 4 indicates the profile of time-averaged solid volume fraction outlined in the radial position at height of 0.4 m by Gidaspow and Wen-Yu drag models.

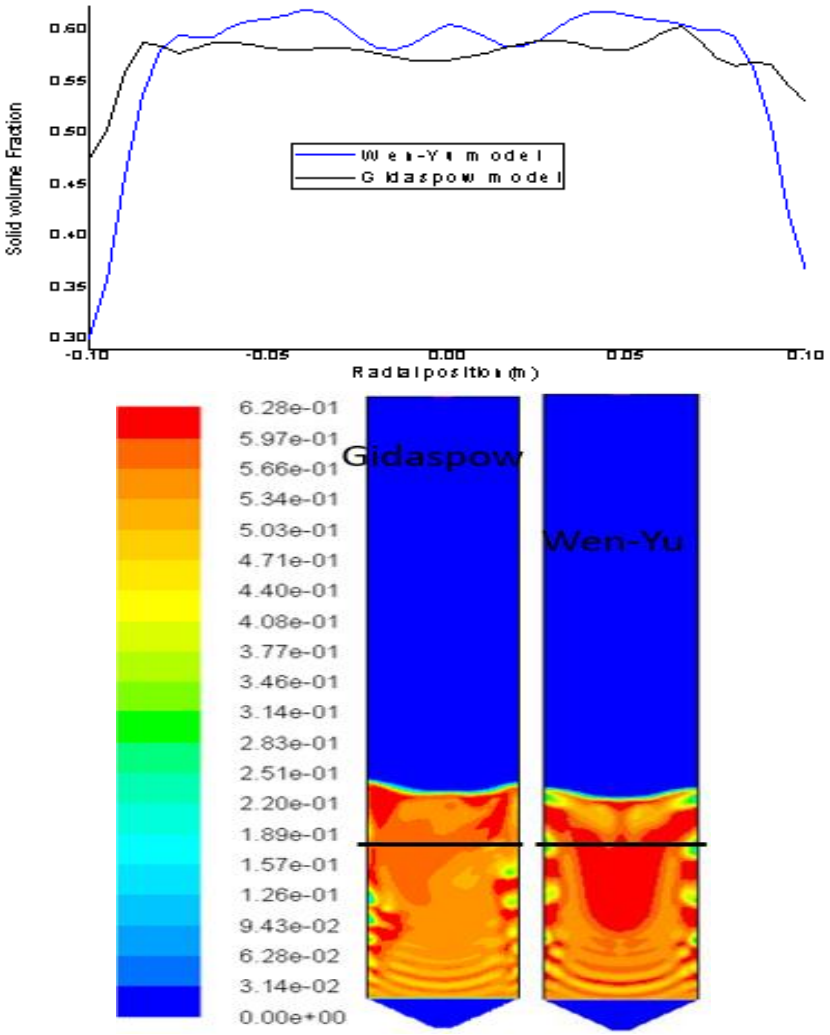

Figure 4. Time-averaged (10 s) simulation of solid (a) volume fraction change along the circular position at 0.4 m of column height and (b) particle volume fraction contour in the fluidized column.

The solids volume fraction shows even distribution along the radial direction for both models, while Wen-Yu model indicates comparatively larger variation of solids volume fraction along the radial direction as compared to Gidaspow model. To conclude from the aforementioned three figures, Gidaspow model seems to be preferable to We-Yu model as it indicates less variation along the radial and axial direction in gas and solid velocity. Also, literature studies (Sahoo and Sahoo, 2015; Loha et al., 2012; Hooyar et al., 2012) appreciate Gidaspow model for evaluation with investigational data. It must also be noted that the Gidaspow model is a modification of Ergun and Wen-Yu models.

Residence time distribution (RTD) validation

The species transport model in ANSYS Fluent® used for the simulation of set time delivered (RTD) is implemented for the fluidized bed in 2D and 3D, respectively. In the RTD study, helium gas is considered as tracer gas. The concentration of the gas is measured when it is leaving, and the residence time predictions are given as

Mean time distribution: $\bar{t} = \frac{\sum c_i t_i \Delta t_i}{\sum c_i \Delta t_i}$ (33)

Exit time distribution: $E(t) = \frac{c(t)}{\sum c_i \Delta t_i}$ (34)

Three cases with air velocities ranging from 6.4 to 9.5 times the minimum fluidization velocity are simulated in this presented work. That means they are indicated as ratio of U_0 / U_{mf} which is 0.634 cm/s. In all the three cases $(U_0 / U_{mf} = 9.5; 8.0 \text{ and } 6.4)$, both the 2D and

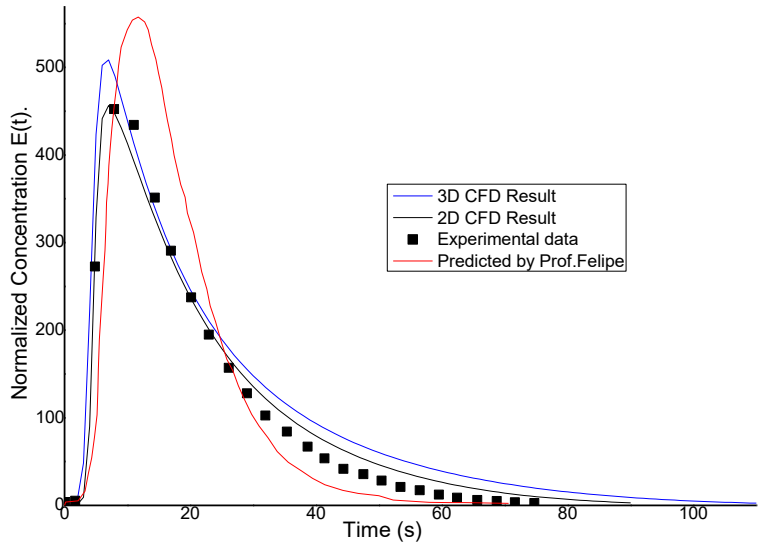

Figure 5. Experimental and predicted RTD response of the fluidized bed under normalized velocity conditions $(U_0/U_{mf}=9.5)$.

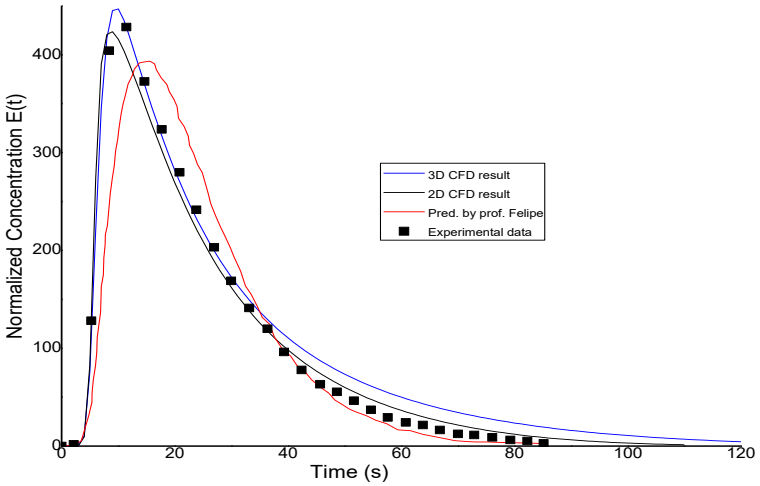

Figure 6. Experimental and predicted RTD response of the fluidized bed under normalized velocity conditions $(U_0/U_{mf}=8.0)$.

3D simulation results are in line with the experimental data (Figures 5 to 7, respectively) especially at lower simulation times; while it seems to over-predict the experimental data as the simulation time proceeds in the end. This is probably because of the numerical discrepancies associated with the CFD model while obtaining the final tracer concentration at the outlet. However, the peaks from the experimental data fit well with the numerical model, although the peaks from the 2D simulations are slightly lower than the peaks from the 3D simualtions. This is probably because in 3D, tracer has enough space to pass through the fluidized bed.

The validation of residence time distribution studies seems to be in line with the experimental study of Lopez-Isunza (1975) for the three different velocity conditions investigated (Figures 5 to 7). The theoretical mean residence time of the air in column is predicated in Kunii and Levenspiel (1991) as $\bar{t}=\dfrac{\alpha_g h_g}{U_0}$. The results are summarized in Table 2 for an initial solids bed height of 0.5 m.

For $U_0/U_{mf}=9.5$, the average residence time is the

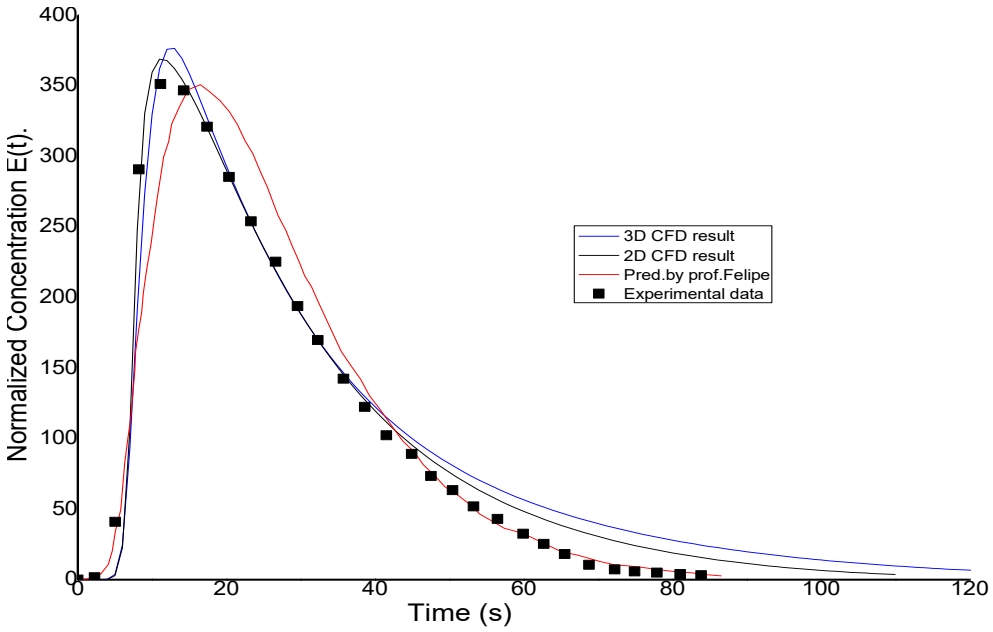

Figure 7. Experimental and predicted RTD response of the fluidized bed under normalized velocity conditions $(U_0 / U_{mf} = 6.4)$.

Table 2. Summary of the numerical outcomes of the mean residence time, compared with results from Lopez-Isunza (1975) and Levenspiel (1999).

Fluidized bed column height, H (m)	Normalized velocity	Mean residence time (s) (Lopez-Isunza, 1975)		Theoretical mean residence time (s) (Levenspiel, 1999)	CFD mean residence time (s)	
		Experiment	Predicted		2D	3D
1.5	9.5	19	14.05	20	22	24.13
1.5	8.0	23.297	18.796	25.490	25.3	28.8
1.5	6.4	25.402	22.320	31.707	29.5	33

fastest (compared to $U_0 / U_{mf} = 6.4$ which is the slowest), which means that the mass transfer between the bubbles and emulsions phase is comparatively faster.

Conclusion

The gas-solid hydrodynamics using computation fluid dynamics (CFD) is important to identify the rate behavior of the inner fluidized column. The CFD implemented in this simulation work is a Eulerian-Eulerian multiphase flow fixed with the kinetic theory of granular flow and standard turbulence model used for closure. The two drag models, necessary for gas-solid interchange coefficient, that is, the Gidaspow and Wen-Yu models, simulate the gas-solids mixing in the bed. Although there is not much difference between the performance of these two models, Gidaspow model is recommended as it is able to correctly capture the hydrodynamics inside the fluidized bed. The simulations results studied are time-averaged distributions of gas and solids velocity along the axial and radial directions. The simulation results related to residence time distribution (RTD) for three different velocity rations $(U_0 / U_{mf} = 9.5; 8.0 \text{ and } 6.4)$, that is, at different degrees of gas-solids mixing, are evaluated in both 2-D and 3-D. The results are similar with the investigational data of Lopez-Isunza (1975). However, further research is still needed to understand the mass transport among the bubble and emulsion phases and connect them to the gas-solid hydrodynamics. It is important to investigate the relation between the mass transport and the residence time distribution, to have a meaningful fluidized column reactor.

CONFLICT OF INTERESTS

The author has not declared any conflict of interests.

REFERENCES

Andreux R, Petit G, Hemati M, Simonin O (2008). Hydrodynamic and solid residence time distribution in a circulating fluidized bed: Experimental and 3D computational study. Chemical Engineering and Processing: Process Intensification 47(3):463-473.

Balakin B, Hoffmann AC, Kosinski P (2012). The collision efficiency in a shear flow. Chemical Engineering Science 68(1):305-312.

Benzarti S, Mhiri H, Bournot H (2012). Drag models for simulation gas-solid flow in the bubbling fluidized bed of FCC particles. World Academy of Science, Engineering and Technology 61:1138-1143.

Chapman S, Cowling TG (1970). The mathematical theory of non-uniform gases: an account of the kinetic theory of viscosity, thermal conduction and diffusion in gases. Cambridge University Press.

Chiba T, Kobayashi H (1970). Gas exchange between the bubble and emulsion phases in gas-solid fluidized beds. Chemical Engineering science 25(9):1375-1385.

Cui H, Grace JR (2007). Fluidization of biomass particles: A review of experimental multiphase flow aspects. Chemical Engineering Science 62(1-2):45-55.

Dutta A, Ekatpure RP, Heynderickx GJ, de Broqueville A, Marin GB (2010). Rotating fluidized bed with a static geometry: Guidelines for design and operating conditions. Chemical Engineering Science 65(5):1678-1693.

Geldart D (1973). Types of gas fluidization. Powder Technology *7*(5):285-292.

Gidaspow D (1994). Multiphase flow and fluidization: continuum and kinetic theory descriptions. Boston: Academic Press.

Gidaspow D, Jung J, Singh RK (2004). Hydrodynamics of fluidization using kinetic theory: an emerging paradigm. Powder Technology 148(2-3):123-141.

Hu X, Zhang J, Dong C, Yang Y (2010). Simulation of Dense Gas-Solid Fluidized Bed Based on Two-Fluid Model. In 2010 Asia-Pacific Power and Energy Engineering Conference (pp. 1-4). IEEE.

Hua L, Wang J, Li J (2014). CFD simulation of solids residence time distribution in a CFB riser. Chemical Engineering Science 117:264-282.

Idakiev V, Morl L (2013). Study of Residence Time of Disperse Materials in Continuously Operating Fluidized Bed Apparatus. Journal of Chemical Technology and Metallurgy *48*(5):451-456.

Kobayashi H, Arai F, Sunagawa T (1967). Kagaku Kogaku (Chemical Engineering, Japan) 29:858.

Kunii D, Octave L (1991). Fluidization Engineering. 2. ed. Butterworth-Heinemann Series in Chemical Engineering. Boston: Butterworth-Heinemann.

Levenspiel O (1999). Chemical reaction engineering (3rd ed). New York: Wiley.

Li P, Lan X, Xu C, Wang G, Lu C, Gao J (2009). Drag models for simulating gas–solid flow in the turbulent fluidization of FCC particles. Particuology *7*(4):269-277.

Loha C, Chattopadhyay H, Chatterjee PK (2012). Assessment of drag models in simulating bubbling fluidized bed hydrodynamics. Chemical Engineering Science 75:400-407.

Lopez-Isunza F (1975). Determination of interchange parameter in fluidized beds using pulse testing techniques. M.Eng Thesis, McMaster University, Canada.

Pant HJ, Sharma VK, Goswami S, Samantray JS, Mohan IN, Naidu T (2014). RTD in a pilot-scale gas–solid fluidized bed reactor using radiotracer technique. Journal of Radioanalytical and Nuclear Chemistry 302(3):1283-1288.

Richardson JF, Harker JH, Coulson JM, Richardson JF (2008). Particle technology and separation processes (5. ed.). Oxford: Butterworth Heinemann.

Sahoo P, Sahoo A (2015). A Comparative Study on Effect of Different Parameters of CFD Modeling for Gas–Solid Fluidized Bed. Particulate Science and Technology 33(3):273-289.

Salaices E, de Lasa H, Serrano B (2012). Steam gasification of a cellulose surrogate over a fluidizable Ni/α-alumina catalyst: A kinetic model. AIChE Journal 58(5):1588-1599.

Schaeffer DG (1987). Instability in the evolution equations describing incompressible granular flow. Journal of Differential Equations 66(1):19-50.

Shi X, Sun R, LAN X, Liu F, Zhang Y, GAO J (2015). CPFD simulation of solids residence time and back mixing in CFB risers. Powder Technology 271:16-25.

Syamlal M, Rogers W, O'Brien TJ (1993). MFIX documentation. National Energy Technology Laboratory, Department of Energy, Technical Note No. DOE/MC31346-5824.

Taghipour F, Ellis N, Wong C (2005). Experimental and computational study of gas–solid fluidized bed hydrodynamics. Chemical Engineering Science 60(24):6857-6867.

Tartan M, Gidaspow D (2004). Measurement of granular temperature and stresses in risers. AIChE Journal 50(8):1760-1775.

Wen CY, Yu YH (1966). Mechanics of Fluidization. Chemical engineering progress symposium series 62:100-111.

Xia B. Sun DW (2002). Applications of computational fluid dynamics (CFD) in the food industry: a review. Computers and Electronics in Agriculture 34(1):5-24.